Experimental Hematology

Experimental Hematology 2019;79:3–15

REGULAR SUBMISSION

KRas^{G12D} expression in the bone marrow vascular niche affects hematopoiesis with inflammatory signals

Cindy L. Hochstetler[a,b], Yuxin Feng[a], Mehmet Sacma[c], Ashley K. Davis[a], Mahil Rao[d], Chia-Yi Kuan[e], Li-Ru You[f,g], Hartmut Geiger[a,c], and Yi Zheng[a,b]

[a]*Division of Experimental Hematology and Cancer Biology, Cincinnati Children's Hospital Medical Center, Cincinnati, Ohio;* [b]*Department of Pathology and Laboratory Medicine, University of Cincinnati, Cincinnati, Ohio;* [c]*Institute of Molecular Medicine and Stem Cell Aging, University of Ulm, Ulm, Germany;* [d]*Division of Pediatric Critical Care, Department of Pediatrics, Stanford University, Stanford, California;* [e]*Department of Neuroscience, University of Virginia, Charlottesville, Virginia;* [f]*Institute of Biochemistry and Molecular Biology, National Yang-Ming University, Taipei, Taiwan;* [g]*Cancer Progression Research Center, National Yang-Ming University, Taipei, Taiwan*

(Received 20 August 2019; revised 14 October 2019; accepted 16 October 2019)

The bone marrow (BM) niche is an important milieu where hematopoietic stem and progenitor cells (HSPCs) are maintained. Previous studies have indicated that genetic mutations in various components of the niche can affect hematopoiesis and promote hematologic abnormalities, but the impact of abnormal BM endothelial cells (BMECs), a crucial niche component, on hematopoiesis remains incompletely understood. To dissect how genetic alterations in BMECs could affect hematopoiesis, we have employed a novel inducible Tie2-CreERT2 mouse model, with a tdTomato fluorescent reporter, to introduce an oncogenic KRas^{G12D} mutation specifically in the adult endothelial cells. Tie2-CreERT2;KRas^{G12D} mice had significantly more leukocytes and myeloid cells in the blood with mostly normal BM HSPC populations and developed splenomegaly. Genotyping polymerase chain reaction revealed KRas^{G12D} activation in BMECs but not hematopoietic cells, confirming that the phenotype is due to the aberrant BMECs. Competitive transplant assays revealed that BM cells from the KRas^{G12D} mice contained significantly fewer functional hematopoietic stem cells, and immunofluorescence imaging showed that the hematopoietic stem cells in the mutant mice were localized farther away from BM vasculature and closer to the endosteal area. RNA sequencing analyses found an inflammatory gene network, especially tumor necrosis factor α, as a possible contributor. Together, our results implicate an abnormal endothelial niche in compromising normal hematopoiesis.

Germ line or acquired mutations in genes of the Rasopathy pathway are often associated with hematologic abnormalities, and patients that harbor such mutations are at an increased risk of developing blood disorders [1]. In fact, in juvenile myelomonocytic leukemia (JMML), Rasopathy mutations have been implicated in ~85% of clinical cases, with a *Ras* mutation being present in about 25% of all cases [2–6]. Mutations in *Kras, Nras, Nf1*, and *Ptpn11* can promote cellular transformation and lead to the development of myeloproliferative disorders (MPDs) and/or myelodysplastic syndromes (MDSs) [7,8] that affect hematopoietic cell output. A study using the interferon-inducible Mx1-Cre mouse model to overexpress *Ptpn11* in the hematopoietic stem and progenitor cells (HSPCs) led to the development of a fatal MPD and anemia [9]. Loss of heterozygosity in the *Nf1* tumor suppressor gene is associated with JMML. The transplantation of fetal *Nf1*$^{-/-}$ HSPCs into recipient mice led to an MPD phenotype that

Offprint requests to: Yi Zheng, Experimental Hematology and Cancer Biology, 240 Albert Sabin Way, Cincinnati, OH 45229; E-mail: yi.zheng@cchmc.org

Supplementary material associated with this article can be found in the online version at https://doi.org/10.1016/j.exphem.2019.10.003.

https://doi.org/10.1016/j.exphem.2019.10.003

mimicked human JMML, suggesting that such mutations can be causal for the clonal expansion of aberrant HSPCs in JMML [10]. Significantly, oncogenic $KRas^{G12D}$ expression resulted in a lethal myeloproliferative disorder with 100% penetrance [11]. These studies suggest that deregulated Ras signaling can promote hematologic abnormalities [1].

HSPCs, which are responsible for hematopoietic cell production, are maintained in a specialized bone marrow microenvironment, the niche [12,13]. Anatomically and functionally defined, the bone marrow niche constitutes a home where HSPCs reside and their balance between self-renewal and differentiation is governed by a host of cell intrinsic and extrinsic factors [14–17]. The existence of several niche components, including the osteoblastic [18,19] and vascular cells [20], has been well documented. These niche cells help maintain and regulate the hematopoietic landscape within the bone marrow and in peripheral blood in a dynamic fashion. Different models have been proposed regarding how niche abnormalities may contribute to blood disease pathogenesis [21]. Several groups have found that genetic mutations in the BM niche cells can lead to the development of myeloproliferative disorders. Mice without retinoic acid γ or with inactivated retinoblastoma protein in their hematopoietic system developed MPD [22,23], whereas deletion of the endonuclease *Dicer1* in mesenchymal osteoprogenitors initiated an MDS-like disease [24]. The activation of mutated *Ptpn11* in Nestin+ cells resulted in increased myeloid progenitors in the bone marrow and increased myeloid cells in the blood [25]. These studies thus indicate that blood abnormalities can be derived from niche anomalies. However, although it is increasingly recognized that bone marrow endothelial cells (BMECs) act as a major niche component required for HSPC interaction [26–29], the functional and mechanistic relationship between an abnormal endothelial niche and blood pathogenesis remains unclear.

In this study, we crossed previously described inducible Tie2Cre-ER mice [30] with mice bearing the conditional lox-stop-lox $KRas^{G12D}$ mutation to specifically introduce a $KRas^{G12D}$ mutation into adult endothelial cells. We also introduced a fluorescent tdTomato reporter to track our genetic mutation. We describe how such a mutation in the vascular niche affects normal hematopoiesis. The mutant mice displayed splenomegaly and decreased HSC reconstitution potential. Molecularly, we observed a surprising inflammatory signature in the BMECs expressing $KRas^{G12D}$. Our findings demonstrate that an altered BM vascular niche can change HSC function and imply that oncogenic KRas may elicit an inflammatory response in the BMECs, contributing to hematologic abnormalities.

Methods

Animals

All animal work was performed in accordance with the protocols approved by the Institutional Animal Care and Use Committee at Cincinnati Children's Hospital Medical Center. To induce Cre expression, male and female mice at the adult stage (6–10 weeks of age) were injected with tamoxifen (Cayman Chemical 13258) for 4 consecutive days. More details are available in the Supplementary Material (online only, available at www.exphem.org

Cell preparation

BM cells were harvested from femurs, tibias, and iliac crests. The bones and spleens were flushed and/or crushed and filtered, and single-cell suspensions were made. For cell sorting, the BMECs were flushed with Hank's balanced salt solution, 2% fetal bovine serum, and 2 mmol/L ethylenediamine tetraacetic acid (EDTA).

Data availability

RNA sequencing data from the sorted CD31+ tdT+ BMECs have been deposited to the National Center for Biotechnology Information's Gene Expression Omnibus (GSE137649).

Statistical analysis

Statistical analyses were performed using GraphPad Prism software. Unless otherwise specified, unpaired Student's t-test and a normal analysis of variance were used. Data were expressed as the mean ± the standard error of the mean. A p value of <0.05 was considered statistically significant.

Additional methods are described in the Supplemental Materials.

Results

$KRas^{G12D}$ expression in the murine bone marrow microenvironment causes an MPD-like phenotype and lethality

To determine the effect of an oncogenic gene mutation on the hematopoietic system, we used an Mx1-Cre; $KRas^{G12D}$ mouse model. The mutant mice showed a drastic increase in total white blood cell counts (Supplementary Figure E1A, online only, available at www.exphem.org). They had increased neutrophil and monocyte counts (Supplementary Figures E1B and E1C), but no change in lymphocyte counts (Supplementary Figure E1D). Overall, they had more myeloid cells, especially in the neutrophil population (Supplementary Figures E1E and E1F), with a concurrent decrease in lymphocyte percentage (Supplementary Figure E1G). Blood smears confirmed the presence of more leukocytes and polychromasia cells (Supplementary Figures E1H and E1I). The mutant mice also had reduced hemoglobin (Supplementary Figure E1J) and platelets (Supplementary Figure E1K). These observations are consistent with previously published results of $KRas^{G12D}$ expression in the broad hematologic compartments leading to MPDs [31].

To examine the effect of $KRas^{G12D}$ expression in the BM microenvironment on hematopoiesis, we transplanted whole BM cells from syngeneic WT CD45.1 BoyJ cells into lethally irradiated adult CD45.2 Mx1-Cre;$KRas^{G12D}$ (WT:KRas) or Mx1-Cre;$KRas^{WT}$ (WT:WT) recipients (Figure 1A).

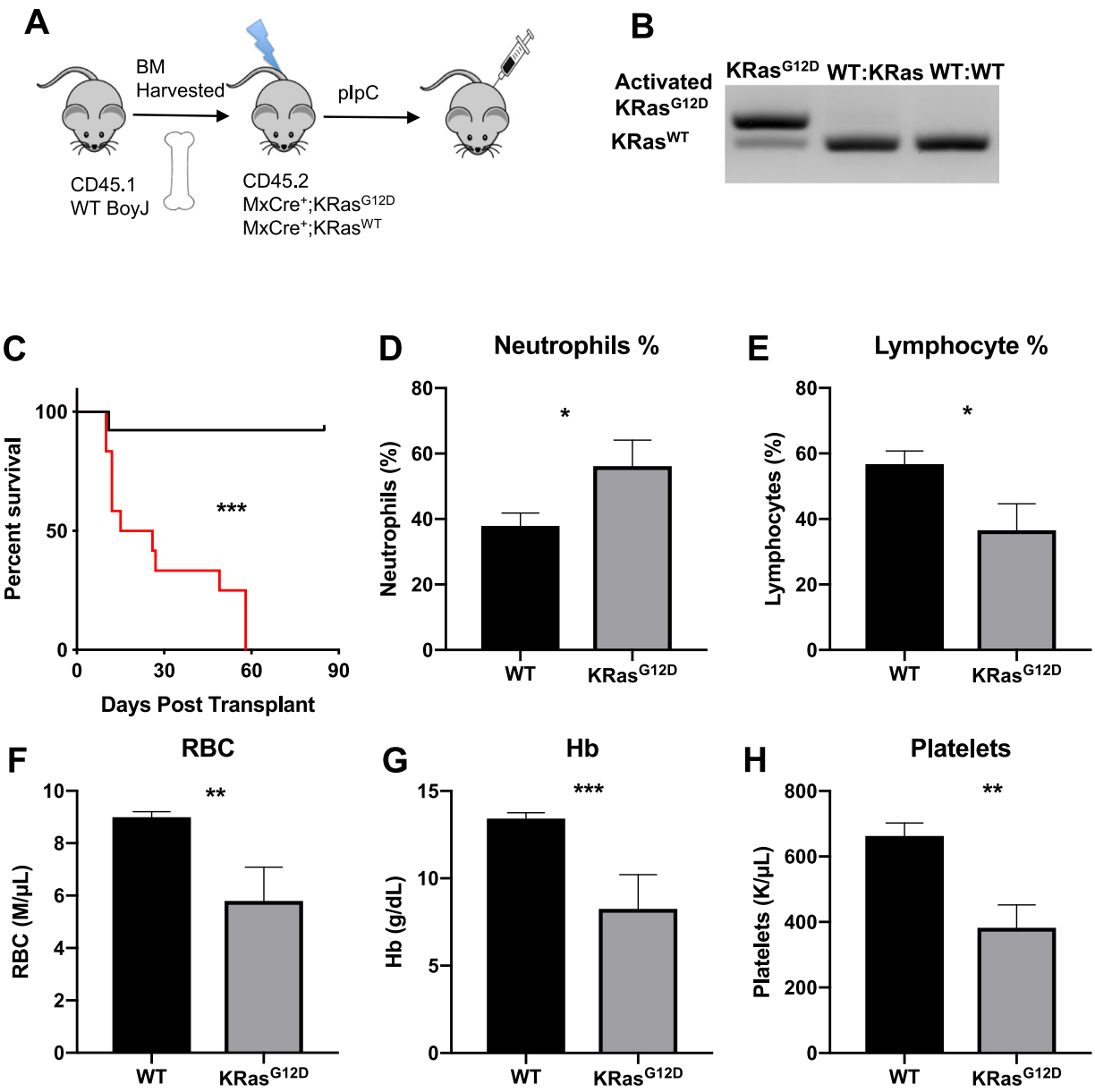

Figure 1. Inducible KRas^{G12D} expression in the BM microenvironment causes an MPD-like phenotype. **(A)** Five million whole BM cells from WT mice were transplanted into lethally irradiated MxCre;KRas^{G12D} or control mice. The recipients were injected with pIpC 1–2 weeks later to induce KRas^{G12D} activation. **(B)** Genotyping data reveal the presence of only WT allele in the mononuclear blood cells of WT:WT and WT:Kras transplanted mice 5 weeks after transplantation. KRas^{G12D} lane: Mononuclear cells from MxCre;KRas^{G12D} mice prior to transplant; WT:KRas lane: WT donor transplanted to a MxCre;KRas^{G12D} recipient; WT:WT lane: WT donor transplanted into a WT recipient. **(C)** Survival curve depicting the faster death of WT:KRas recipients. Complete blood counts by Hemavet (Drew Scientific) revealed an increase in the percentage of **(D)** neutrophils with concurrent decrease in **(E)** lymphocytes, as well as **(F, G)** anemia development and **(H)** decreased platelet counts. $n = 6–12$. *$p < 0.05$. **$p < 0.01$. ***$p < 0.001$.

Genotyping polymerase chain reaction (PCR) analysis of the peripheral blood cells after poly(I:C) injection of KRas^{G12D} recipient mice revealed the absence of activated KRas^{G12D}, suggesting that the observed effect was due to KRas^{G12D} expression in the nonhematologic lineage microenvironment (Figure 1B). A Kaplan–Meier log-rank test showed that WT:KRas mice all died within 100 days after transplantation, whereas all but one of the WT:WT recipients remained alive at the end of the period (Figure 1C). Five weeks post-transplantation, blood composition was found unchanged in the WT:WT recipients, but the WT:KRas mice rapidly developed a myeloproliferative phenotype, as evidenced by the increased percentage of neutrophils in the blood (Figure 1D) and concurrent decrease in the percentage of lymphocytes (Figure 1E). We also observed rapid anemia and thrombocytopenia onsets in the WT:KRas mice, as they had significantly

lower counts of red blood cells (Figure 1F), hemoglobin (Figure 1G), and platelets (Figure 1H). Thus, $KRas^{G12D}$ expression in the BM microenvironment is sufficient to cause an MPD-like phenotype and lethality.

An inducible, endothelial cell-specific $KRas^{G12D}$-expressing mouse model

The effects of genetic mutations in BM niche components have been intensively studied recently, and it has been shown that these mutations can induce hematologic malignancies [24,25]. Endothelial-specific knockout of SCF or CXCR4 has also been reported to alter the BM microenvironment for HSC maintenance [32,33]. To investigate how a genetic mutation, such as $KRas^{G12D}$, when restricted in BMECs, may alter the BM microenvironment and possibly affect hematopoiesis, we utilized a recently generated inducible Tie2-CreERT2 mouse model allowing expression of genes selectively in adult mice ECs. This mouse model is highly efficient in response to tamoxifen injection to express Cre activity only in the endothelial lineage, not blood lineages [34]. Six- to ten-week-old adult Tie2-CreERT2;$KRas^{G12D}$ mice, denoted as $KRas^{G12D}$ mice, and control Tie2-CreERT2;$KRas^{WT}$, denoted as WT mice, were injected with TAM. This led to specific activation of oncogenic KRas in endothelial cells (Figure 2A). We tracked the tdTomato (tdT) fluorescent reporter to confirm the specific activation of $KRas^{G12D}$ in endothelial cells. Immunofluorescence staining revealed that the fluorescent reporter was strictly confined in the vasculature, which expressed endothelial marker CD31 (Figure 2B–D), and co-localized with the endothelial markers Ve-Cadherin, VEGFR2, and DiI-Ac-LDL labeled BM sinusoids [35] (data not shown). Immunofluorescence staining of flushed BM showed similar vascular expression of the tdT marker in WT and mutant mice (Figure 2E, F). FACS analysis also showed no difference in the CD31+tdT+ cell frequencies in WT and mutant bone marrow or spleen (Figure 2G, H). To exclude the possibility that the induced phenotype might be due to gene leakage in the hematopoietic system, we seeded BM cells into M3434 Methocult medium and isolated the colonies 7–10 days later. Genotyping PCR found activated $KRas^{G12D}$ allele in the CD31+tdT+ endothelial cells but not in the hematopoietic cells (Figure 2I–K). We thus utilized this new mouse model to study the effect of the $KRas^{G12D}$ mutation in BMECs on hematopoiesis.

Endothelial cell-specific $KRas^{G12D}$ expression leads to leukocytosis and myeloid bias

Following TAM injection, retro-orbital bleeds were performed monthly to assess blood composition. The $KRas^{G12D}$ mice develop leukocytosis, as the absolute counts of both myeloid and lymphoid cells increased (Figure 3A–D). Fluorescence-activated cell sorting (FACS) analysis revealed a myeloid versus lymphoid cell bias as evidenced by an increase in the percentage of myeloid cells (Figure 3E–G) and a decrease in the percentage of lymphocytes (Figure 3H).

To further ensure the Tie2-CreERT2;$KRas^{G12D}$ model limited $KRas^{G12D}$ expression in the endothelia, we transplanted WT CD45.1 whole BM cells into lethally irradiated CD45.2 $KRas^{G12D}$ (WT:KRas) or $KRas^{WT}$ (WT:WT) recipients, and injected the recipient mice with TAM after engraftment (Supplementary Figure E2A, online only, available at www.exphem.org). Similar to the native Tie2-CreERT2;$KRas^{G12D}$ model, the $KRas^{G12D}$ recipients developed splenomegaly (Supplementary Figure E2B). At 16 weeks post-transplant, the WT:KRas mice had a significantly higher percentage of myeloid cells, especially neutrophils, and a lower percentage of lymphoid cells (Supplementary Figure E2C–F). Furthermore, the KRas:WT recipients showed signs of anemia, as evidenced by a lower hemoglobin count (Supplementary Figure E2G).

To determine the effects on blood composition in $KRas^{G12D}$ mice, we performed FACS analysis to assess the different progenitor compartments in the BM. Our results indicated that most HSPCs appeared normal. There were no major changes within the different LK (Lin−Sca+cKit−) and LSK (Lin−Sca+cKit+) compartments (Figure 4A, B). In addition, colony-forming assays revealed that the BM of $KRas^{G12D}$ mice had slightly increased colony-forming activity (Figure 4C). Pathologic examination of the BM with hematoxylin and eosin (H&E) revealed no major changes (Supplementary Figure E3A, B, online only, available at www.exphem.org). These results indicate that endothelia expression of $KRas^{G12D}$ does not significantly affect HSPC populations and activities in the BM compartments.

On the other hand, the $KRas^{G12D}$ mice exhibited clear splenomegaly (Figure 4D). Endothelial $KRas^{G12D}$ expression altered the hematopoietic composition in the spleen, as the spleens of mutant mice had an increased percentage of myeloid cells (Supplementary Figure E3C), especially neutrophils (Supplementary Figure E3D), with a concurrent decrease in lymphoid cell percentage. However, there was no change in lymphoid cell numbers (data not shown). FACS analysis further showed significant expansion of the GMP population (Figure 4E) and a small increase in the ST-HSC population (Figure 4F). Colony-forming unit (CFU) assays revealed that the $KRas^{G12D}$ spleens had greater colony-forming activity as evidenced by a significantly increased number of CFUs (Figure 4G). CFU activity from the blood of $KRas^{G12D}$ mice was also significantly increased (Supplementary Figure E3E), but it is not clear whether GMP and ST-HSC populations are responsible for the increased colony numbers. Gross

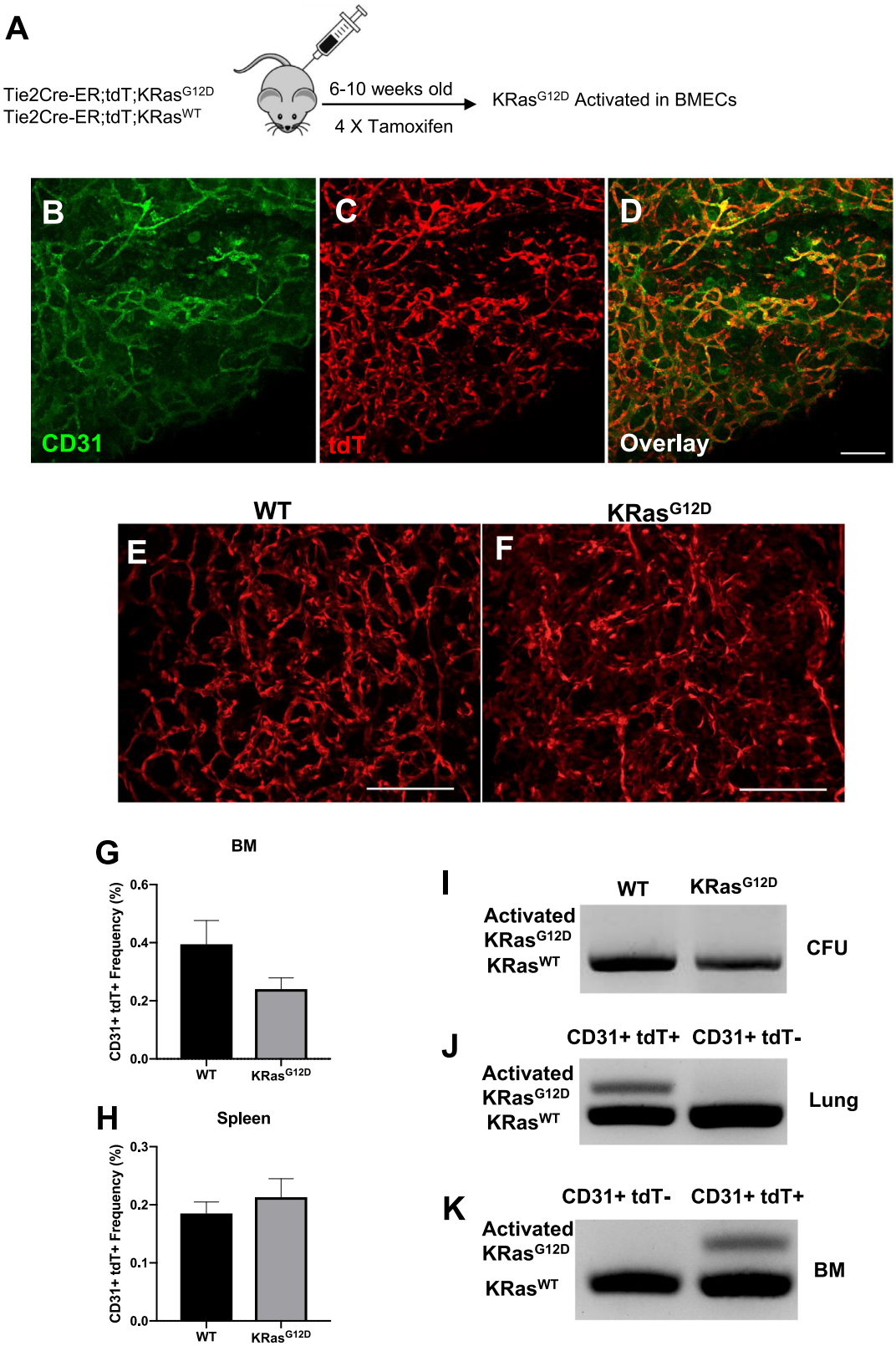

Figure 2. Inducible expression of KRas^{G12D} in the BM endothelial cells of the Tie2-CreERT2 mouse model. **(A)** Schematic representing the model used. **(B–D)** Immunofluorescence staining to determine the expression of CD31 in tdT+ BM after tamoxifen induction. **(B)** CD31 staining. **(C)** tdT. **(D)** Overlay of CD31 and tdT. **(E, F)** Confocal microscopy detected no obvious change in the BM vasculature. **(G, H)** FACS analysis measuring CD31+ tdT+ cell frequency in the **(G)** BM and **(H)** spleen ($n = 5$) of the Tie2-CreERT2 mice. **(I)** Genotyping PCR found no KRas^{G12D} activation in hematopoietic cells assayed from colonies of whole bone marrow cells. **(J, K)** KRas^{G12D} activation is shown in **(J)** freshly sorted CD31+tdT+ lung endothelial cells and **(K)** sorted CD31+tdT+ BM endothelial cells.

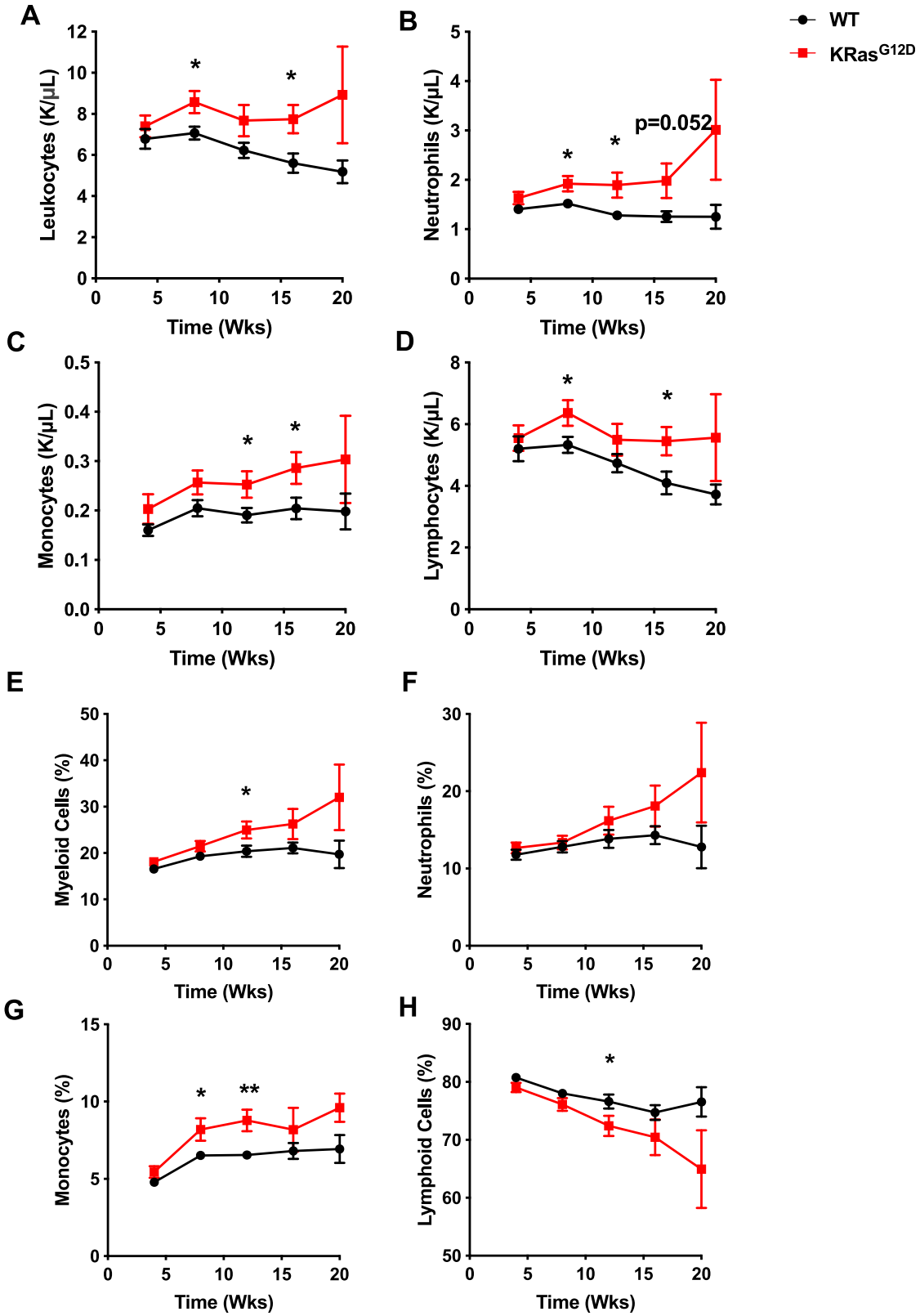

Figure 3. Endothelial KRas^{G12D} expression leads to leukocytosis and myeloid bias. Complete blood counts revealed that KRas^{G12D} mice had higher counts of **(A)** leukocytes, **(B)** neutrophils, **(C)** monocytes, and **(D)** lymphocytes. FACS analysis of the blood also showed an increase in the percentages of **(E)** total myeloid, **(F)** neutrophils, and **(G)** monocytes, with a concurrent decrease in **(H)** lymphocytes. $n \geq 5$. *$p < 0.05$. **$p < 0.01$.

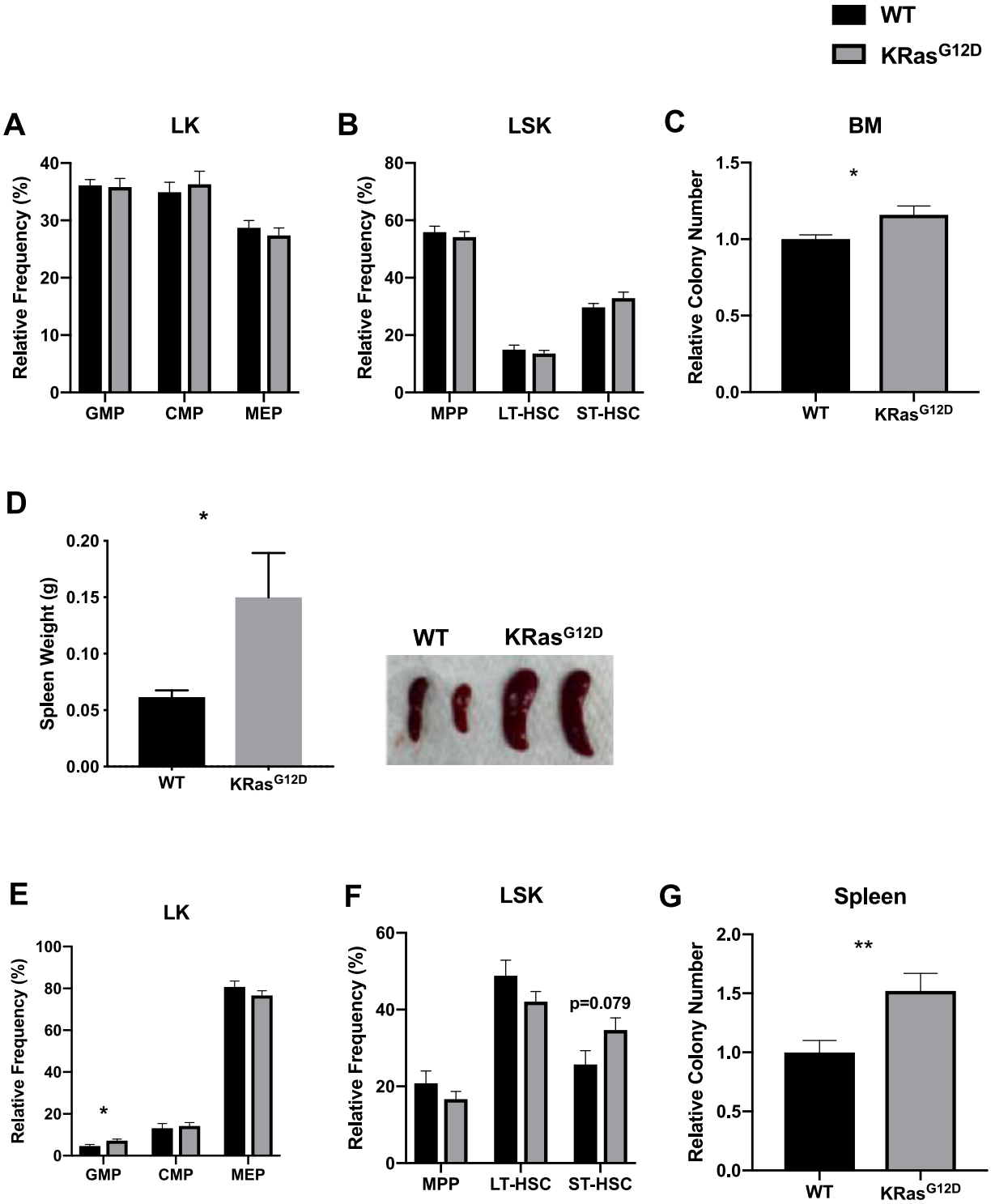

Figure 4. Endothelial $KRas^{G12D}$ expression does not significantly alter the HSPCs in the BM but promotes extramedullary hematopoiesis. FACS analysis of the BM progenitor cells revealed no major change in the **(A)** LK or **(B)** LSK compartments. **(C)** Colonies were scored 7–10 days after total bone marrow cells were plated in Methocult. $n \geq 10$. **(D)** $KRas^{G12D}$ mice had enlarged spleens ($n = 3$ or 4). FACS analysis of spleen progenitor cells revealed **(E)** expansion of the GMP compartment and **(F)** a small increase in the ST-HSC compartments. **(G)** Colonies were scored 7–10 days after spleen cells were plated in Methocult. $KRas^{G12D}$ mice had increased colony-forming potential. $n \geq 10$. $^{*}p < 0.05$. $^{**}p < 0.01$.

examination of the spleen with H&E revealed a slight disruption of the splenic architecture with a modest broadening of the white pulp regions (Supplementary Figure E3F, G). These results suggest that endothelial $KRas^{G12D}$ expression alters extramedullary hematopoiesis in the spleen, which may contribute to the observed myeloid bias and leukocytosis phenotypes.

Endothelial $KRas^{G12D}$ reduces HSC function and alters their BM vascular localization

To determine if there were functional consequences of HSCs residing in an abnormal BM vascular niche, we performed a competitive transplantation experiment followed by a secondary transplantation. At 13 weeks post-TAM injection, we transplanted 2.5 million whole BM cells from pooled CD45.2 $KRas^{G12D}$ (KRas:WT) or $KRas^{WT}$ (WT:WT) mice, along with 2.5 million host supportive cells, into lethally irradiated CD45.1 syngeneic BoyJ primary recipients (Figure 5A). These mice were then bled monthly to assess donor chimerism. FACS analysis revealed that the KRas:WT mice had significantly less overall CD45.2% donor chimerism (Figure 5B) and in all blood lineages analyzed (Figure 5C, D). To analyze the functionality of the HSCs, 5 months after the primary transplantation, the BM cells from the recipients were transplanted into lethally irradiated CD45.1 secondary recipients. FACS analysis revealed an effect similar to that in the primary transplant recipients: 5 months post-transplant, the KRas:WT recipients had significantly reduced overall donor chimerism (Figure 5E) and in all blood lineages analyzed (Figure 5F, G).

To determine if the observed phenotypic and functional abnormality of the HSCs is reflected in their BM niche localization, we examined the endogenous HSCs by immunofluorescence in the native bones harvested 13 weeks post-TAM injections. The HSCs in mutant mice were seen localized more distal to the blood vessels (Figure 6A–D). Quantification revealed that the HSCs of mutant mice were located closer to the endosteal area (Figure 6E) but were significantly further away from the vasculature (Figure 6F).

$KRas^{G12D}$-expressing BM endothelial cells gain an inflammatory signature

As a change in the BM endothelial niche may alter the microenvironment in which HSCs reside, we asked how the BMECs have modified the immediate niche components that may affect the hematopoietic landscape. Thirteen weeks post-TAM injection, WT and mutant mice were euthanized and their BM cells harvested. RNA was obtained from CD31+tdT+ sorted cells and RNA-sequencing (RNA-seq) was performed. The genes were grouped, and differentially expressed pathways were obtained using EGSEA [36] (Figure 7A). Gene set enrichment analysis (GSEA) revealed a list of the differentially expressed genes (Figure 7B). The enrichment plots showed that the cytokine–cytokine receptor interaction pathway and the TNFα signaling pathways were among the most significantly enriched (Figure 7C–E). To further validate these results, CD31+tdT+ cells in the BM were analyzed by FACS and Western blotting for the tumor necrosis factor α (TNFα) level. The $KRas^{G12D}$ mice contained significantly higher TNFα protein in their BMECs (Figure 7F, G). Interestingly, p-ERK and p-AKT levels in the isolated $KRas^{G12D}$-expressing BMECs did not exhibit significant differences from those of the WT samples (Figure 7H), suggesting the growth-promoting MAPK pathway was not altered in the BMECs. Consistently, the mutant BM vasculatures appeared normal compared with that of WT mice (Figure 2E, F), indicating that even under the influence of a strong genetic mutation such as $KRas^{G12D}$, the BM vasculatures strive to retain normal angiogenic activity.

Discussion

HSCs are maintained in a tightly regulated BM niche that contains balanced secreted signals such as cytokines and chemokines. The secretory signals can be modulated by a change in the niche components. Multiple studies using the interferon-inducible Mx1-Cre model have found that an oncogenic KRas mutation in the hematopoietic system could lead to leukocytosis and a phenotype that is reminiscent of MPDs/MDSs [11,37]. To interrogate the contributions of the BM niche components, mutations were introduced into cells of the osteoblastic lineage [18,24] and mesenchymal stroma cells [25,38]. These studies found that oncogenic mutations such as *Dicer* and *Shp2* in these niche cell types are sufficient to cause hematologic malignancies. In our study, WT mouse BM transplantation into Mx1-Cre;$KRas^{G12D}$ mice caused increased myeloid cell bias with a decrease in lymphoid cells. Consistent with what has previously been reported by Staffas et al. [31], our Mx1-Cre;$KRas^{G12D}$ recipient mice with WT blood cells had significantly less hemoglobin and platelets, and developed MPD/MDS-like syndromes that led to lethality. As germ-line and acquired mutations of the Rasopathy pathway have previously been linked with diverse blood disorders [39,40], we seek to understand how an initiating oncogenic $KRas^{G12D}$ mutation in the BMECs alone may affect the normal hematopoietic process. An aberrant BM vascular niche expressing genetic mutations such as $KRas^{G12D}$ led to increased leukocytosis with a myeloid versus lymphoid differentiation bias, which is reminiscent of MPD/MPN. At later time points of our model, this phenotype was even more pronounced, and the mice also developed anemia (data not shown). However, we did not observe a transformation to leukemia, suggesting that a hit such as $KRas^{G12D}$ in the bone marrow endothelial microenvironment is not enough for full transformation.

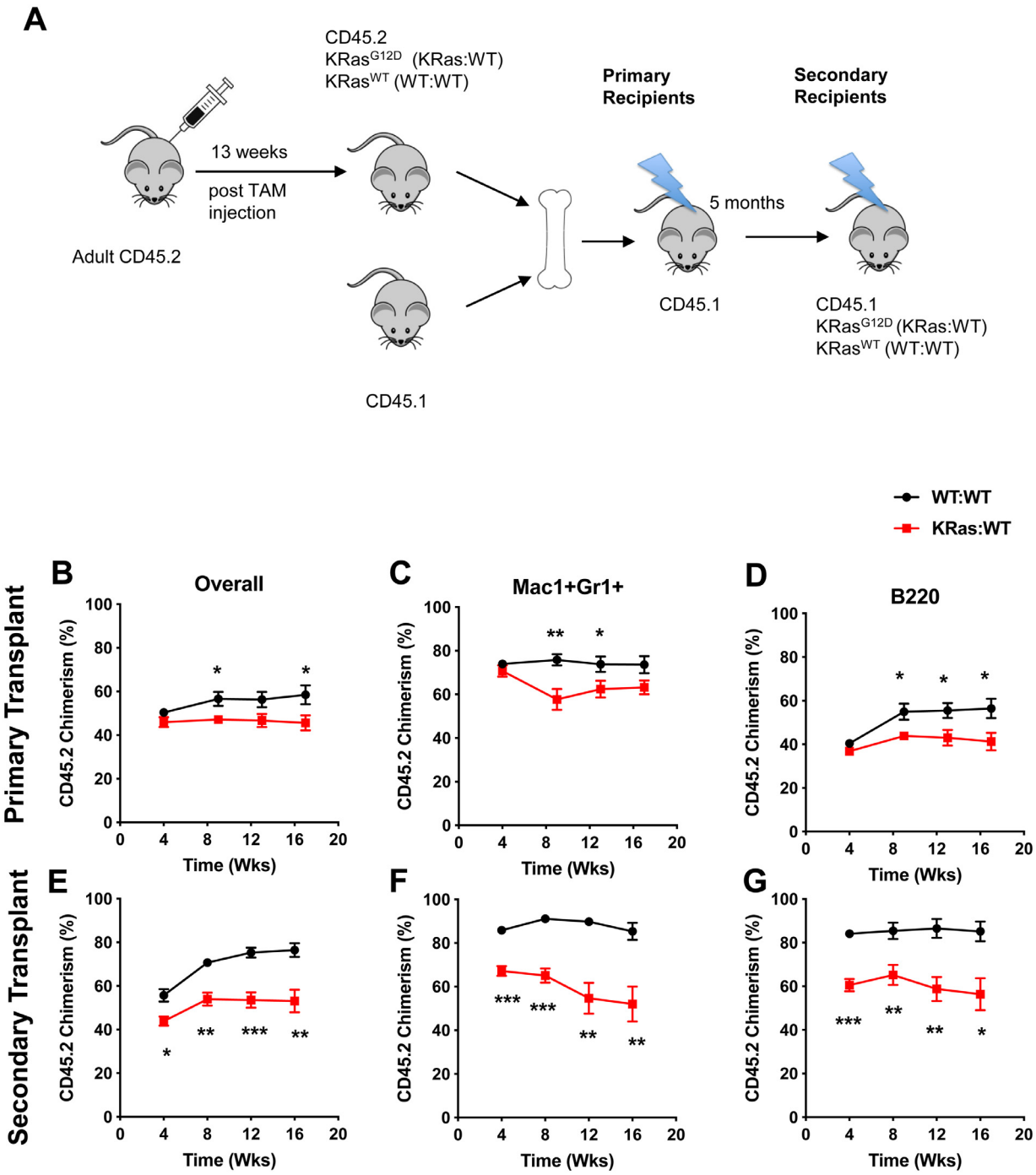

Figure 5. Endothelial KRas^{G12D} expression reduces HSC function. **(A)** Schematic for competitive transplant model. Two and one-half million whole BM cells were transplanted from pooled KRas^{G12D} or WT CD45.2 donors injected with TAM into lethally irradiated syngeneic BoyJ recipients. Two and one-half million CD45.1 cells were also used as competitor cells. Five months later, 3 million cells from pooled donors were transplanted to lethally irradiated syngeneic BoyJ recipients in a noncompetitive setting. Compared with WT:WT, primary KM:WT recipients had **(B)** significantly overall lower CD45.2% donor chimerism and in all blood lineages analyzed, namely, **(C)** Mac1+Gr1+ and **(D)** B220. Compared with WT:WT, secondary KM:WT recipients had **(E)** significantly overall lower CD45.2% donor chimerism and in all blood lineages analyzed, namely, **(F)** Mac1+Gr1+ and **(G)** B220. $n = 5–7$. $^*p < 0.05$. $^{**}p < 0.01$. $^{***}p < 0.001$.

Recent studies have demonstrated that HSCs and progenitors mostly reside close to the BM vasculature, specifically in the perisinusoidal niche [41], which are the exclusive sites for HSPC migration from the BM [42]. Our HSC/BMEC co-imaging data revealed that HSCs of KRas^{G12D} mice were located further from the vasculature but closer to the endosteum. Such a location may explain the observed reduction in HSC

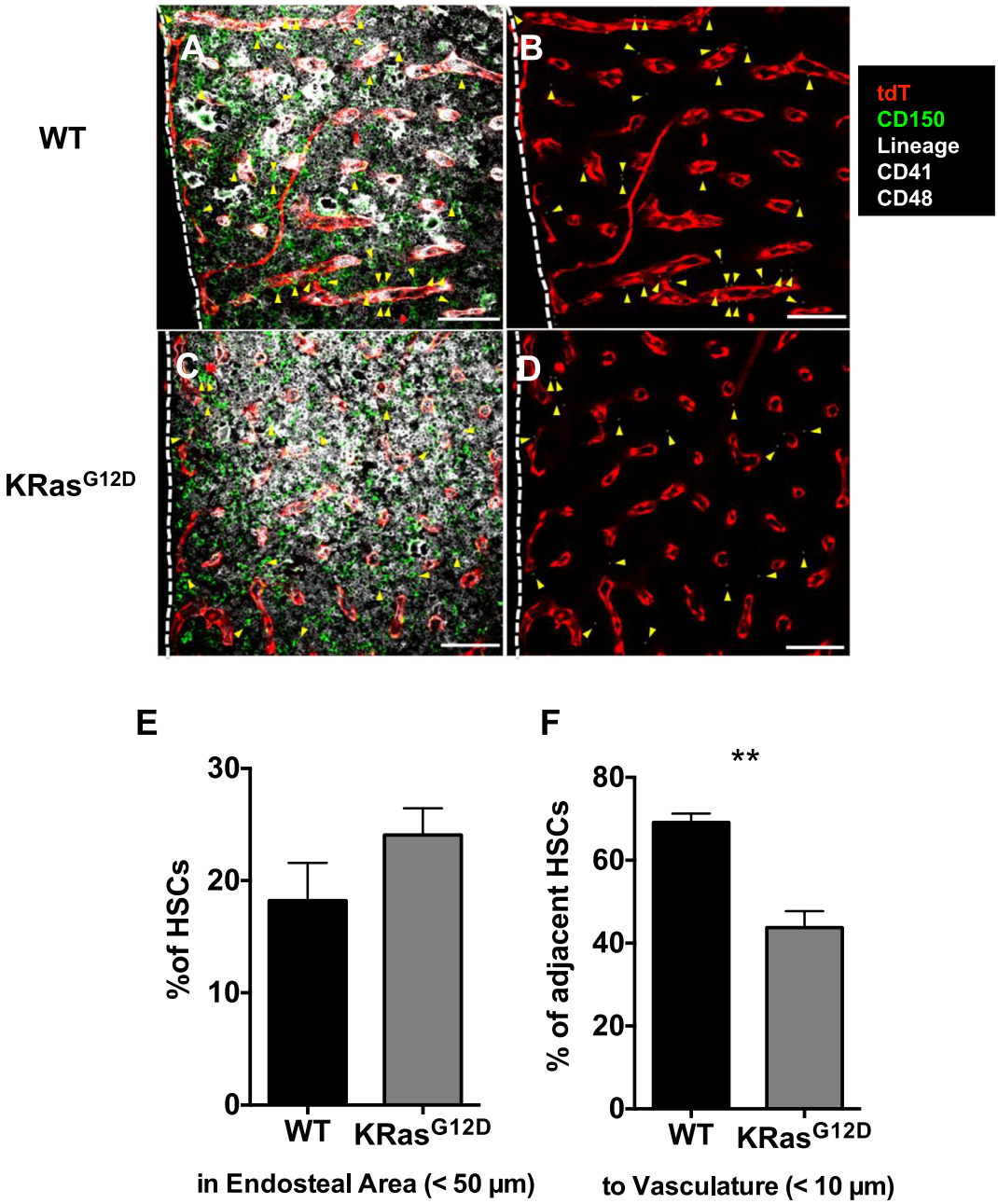

Figure 6. Endothelial KRas^{G12D} alters HSC localization in the BM. **(A–D)** Immunostaining revealed that the mice expressing endothelial KRas^{G12D} had fewer long-term stem cells closer to blood vessels. Quantification showed that in mice expressing endothelial KRas^{G12D}, the HSCs (indicated by the yellow arrowheads) were located slightly closer to the **(E)** endosteal area, but significantly further away from the **(F)** vasculature. $^{**}p < 0.01$.

function of the mutant mice. The observed splenomegaly phenotype in the mutant mice could be a result of more egress of immature HSPCs into the circulation, and it is likely that the altered spleen contributed to the increased leukocytosis.

Interestingly, under homeostatic conditions, while the KRas^{G12D}-expressing BM vasculature appeared normal in morphology and the BMECs did not bear detectable change in canonical MAPK signaling, our RNA sequencing analysis revealed that multiple gene expression changes in the KRas^{G12D}-expressing BMECs occur, with a significant increase in the inflammatory signatures, especially in the TNFα pathway. The cytokine–cytokine receptor interaction network was also significantly enriched. We speculate that the increased TNFα secretion from the mutant BMECs and the resulting inflammatory microenvironment are factors contributing to the hematopoiesis change observed in

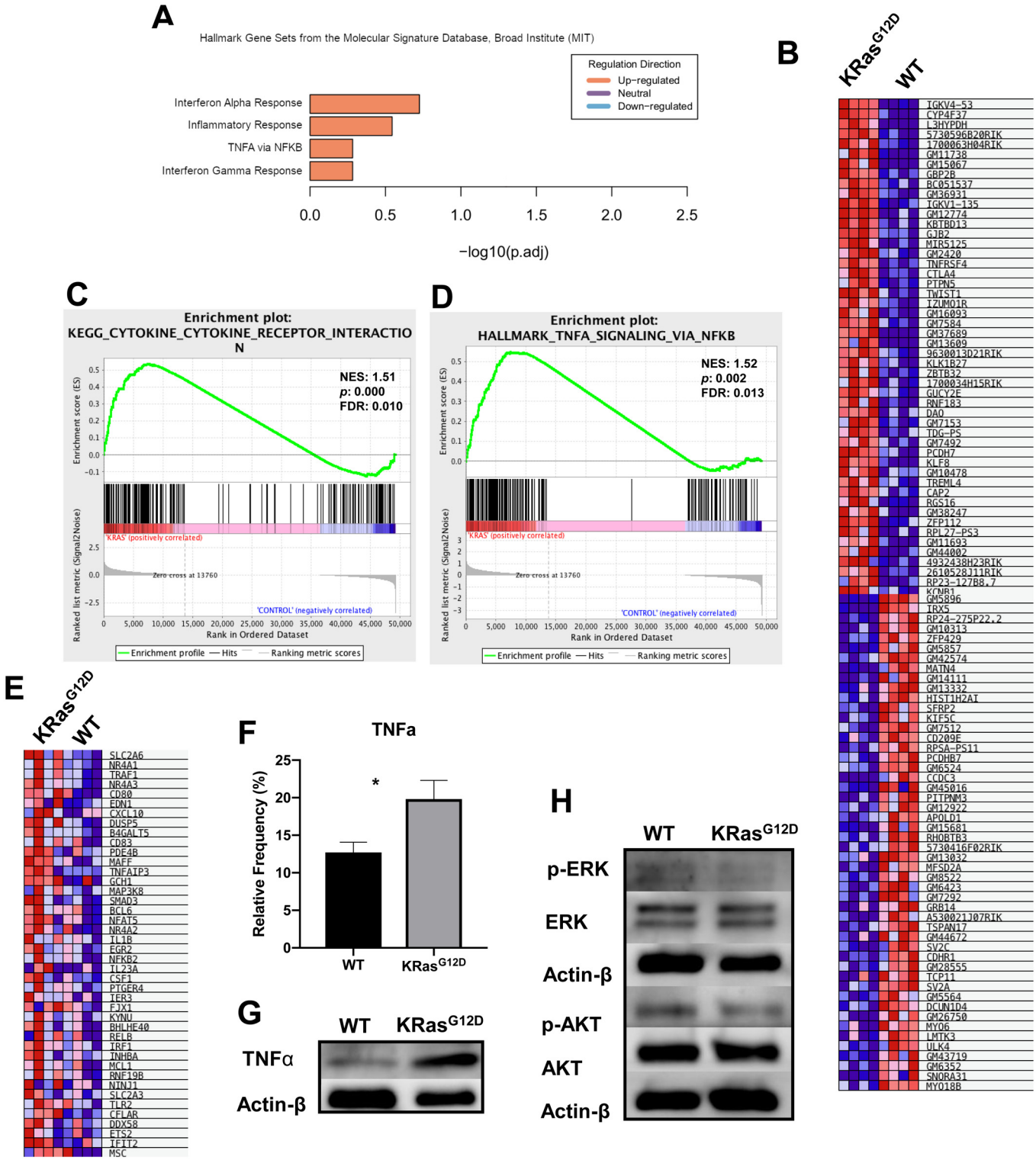

Figure 7. KRas^{G12D} BM endothelial cells contain increased inflammatory signatures. BMECs were sorted on the basis of CD31+tdT+ signals. **(A)** After sequencing, differentially expressed pathways were determined with EGSEA. $n = 4$. **(B)** By use of GSEA software, the most differentially expressed genes were made into a heat map. **(C, D)** Enrichment plots were then generated. **(E)** Heat map revealing the differentially expressed genes within the TNFα pathway. BM cells were harvested, and by use of FACS, CD31+tdT+ cells were assessed for TNFα levels by **(F)** flow cytometry ($n = 5$) and **(G)** Western blot. **(H)** Phospho-ERK and phospho-AKT levels were also assessed. *$p < 0.05$.

the mutant mice. Walkley et al. [22] formerly showed that myeloid proliferation derived from a microenvironment-induced defect was partially caused by a significant increase in TNFα expression. However, similar to their case, we did not observe any significant increase in other cytokines typically linked with inflammation (data not shown). A more recent study by Zhou et al. [43] showed that, in a Fanconi anemia model, WT bone marrow transplantation into $Fancc^{-/-};Fancg^{-/-}$ double knockout mice resulted in significantly decreased colony-forming potential of BM cells, but a marked increase in the myeloid cells and their associated progenitors in a co-culture model. This phenotype was accompanied by a significant increase in TNFα concentration measured from the supernatant of their mesenchymal stem progenitor cells and adipocytes. This suggests that TNFα can contribute to the expansion of myeloid cells. Although the increase in TNFα may partially underlie the BM transplant results that showed a reduced long-term reconstitution capability of the HSCs, it is likely that additional factors in the altered BMEC microenvironment also play important roles as the inflammatory gene changes were more profound. To this end, our results are also consistent with other reports that TNFα had inhibitory effects on hematopoiesis and HSPC exposure to extraneous TNFα pre-transplant impaired HSPC reconstitution capability [44,45].

Previous clinical studies have revealed that abnormal niche components can promote blood disorders. Verstovsek et al. [46] found that the bone marrows of patients with primary myelofibrosis (MF) have a large number of abnormal neoplastic fibrocytes, and transplantation of these BM cells into immunodeficient mice caused the recipient mice to develop a phenotype that resembles MF. Furthermore, a study looking at splenic vascular endothelial cells (SVECs) in MF patients reported that those SVECs may contribute to the expansion of MF CD34+ cells [47]. Additionally, when BM samples were collected from patients with aplastic anemia, researchers found that the BM mesenchymal cells from the patients had an abnormal morphology and appeared "ragged" [48]. These studies thus strongly support the concept that an abnormality in the niche can trigger changes in hematopoiesis.

Taken together, our data provide direct evidence that an alteration in BMECs can abrogate normal hematopoiesis, affecting HSC function and myeloid versus lymphoid lineage balance. As some Ras pathway inhibitors have shown promising results in animal models, our studies suggest that BMECs affected by genetic mutations can be therapeutic targets. Significantly, oncogenic mutations in BMECs may promote an inflammatory surrounding that contributes to blood pathogenesis.

Acknowledgments

We thank the Flow Cytometry Core, the Comprehensive Mouse and Cancer Core, and the Pathology Research Core at Cincinnati Children's Hospital Medical Center for their technical assistance. We also thank James Johnson for technical assistance and Feng Zhang for assistance in obtaining expression counts. This work was supported in part by a Cancer Free Kids grant, a National Institute of Environmental Health Sciences T32ES007250 training grant and a National Heart, Lung, and Blood Institute F31HL136229 training grant to CLH, and National Institutes of Health grants RO1 DK104814, R01 CA204895, and R01 HL134617 to YZ.

Conflict of interest disclosure

The authors have no conflicts of interest to disclose.

Authorship contributions

CLH designed experiments, performed the research, and wrote the article. YF, MS, AKD, and MR performed the research. CYK, LRY, and HG provided crucial reagents. YZ designed experiments and wrote the article.

References

1. Lauchle JO, Braun BS, Loh ML, Shannon K. Inherited predispositions and hyperactive Ras in myeloid leukemogenesis. Pediatr Blood Cancer. 2006;46:579–585.
2. Side L, Taylor B, Cayouette M, et al. Homozygous inactivation of the NF1 gene in bone marrow cells from children with neurofibromatosis type 1 and malignant myeloid disorders. N Engl J Med. 1997;336:1713–1720.
3. Tartaglia M, Niemeyer CM, Fragale A, et al. Somatic mutations in PTPN11 in juvenile myelomonocytic leukemia, myelodysplastic syndromes and acute myeloid leukemia. Nat Genet. 2003;34:148–150.
4. Flotho C, Valcamonica S, Mach-Pascual S, et al. RAS mutations and clonality analysis in children with juvenile myelomonocytic leukemia (JMML). Leukemia. 1999;13:32–37.
5. Kalra R, Paderanga DC, Olson K, Shannon KM. Genetic analysis is consistent with the hypothesis that NF1 limits myeloid cell growth through p21ras. Blood. 1994;84:3435–3439.
6. Loh ML, Reynolds MG, Vattikuti S, et al. PTPN11 mutations in pediatric patients with acute myeloid leukemia: results from the Children's Cancer Group. Leukemia. 2004;18:1831–1834.
7. Janssen JW, Steenvoorden AC, Lyons J, et al. RAS gene mutations in acute and chronic myelocytic leukemias, chronic myeloproliferative disorders, and myelodysplastic syndromes. Proc Natl Acad Sci USA. 1987;84:9228–9232.
8. MacKenzie KL, Dolnikov A, Millington M, Shounan Y, Symonds G. Mutant N-ras induces myeloproliferative disorders and apoptosis in bone marrow repopulated mice. Blood. 1999;93:2043–2056.
9. Chan G, Kalaitzidis D, Usenko T, Kutok JL, Yang W, Mohi MG, et al. Leukemogenic Ptpn11 causes fatal myeloproliferative disorder via cell-autonomous effects on multiple stages of hematopoiesis. Blood. 2009;113:4414–4424.
10. Ingram DA, Wenning MJ, Shannon K, Clapp DW. Leukemic potential of doubly mutant Nf1 and Wv hematopoietic cells. Blood. 2003;101:1984–1986.

11. Braun BS, Tuveson DA, Kong N, et al. Somatic activation of oncogenic Kras in hematopoietic cells initiates a rapidly fatal myeloproliferative disorder. Proc Natl Acad Sci USA. 2004;101:597–602.
12. Schofield R. The relationship between the spleen colony-forming cell and the haemopoietic stem cell. Blood Cells. 1978;4:7–25.
13. Trentin JJ. Determination of bone marrow stem cell differentiation by stromal hemopoietic inductive microenvironments (HIM). Am J Pathol. 1971;65:621–628.
14. Arai F, Hirao A, Ohmura M, et al. Tie2/angiopoietin-1 signaling regulates hematopoietic stem cell quiescence in the bone marrow niche. Cell. 2004;118:149–161.
15. Sacchetti B, Funari A, Michienzi S, et al. Self-renewing osteoprogenitors in bone marrow sinusoids can organize a hematopoietic microenvironment. Cell. 2007;131:324–336.
16. Himburg HA, Harris JR, Ito T, et al. Pleiotrophin regulates the retention and self-renewal of hematopoietic stem cells in the bone marrow vascular niche. Cell Rep. 2012;2:964–975.
17. Zhang J, Grindley JC, Yin T, et al. PTEN maintains haematopoietic stem cells and acts in lineage choice and leukaemia prevention. Nature. 2006;441:518–522.
18. Calvi LM, Adams GB, Weibrecht KW, et al. Osteoblastic cells regulate the haematopoietic stem cell niche. Nature. 2003;425:841–846.
19. Xie Y, Yin T, Wiegraebe W, et al. Detection of functional haematopoietic stem cell niche using real-time imaging. Nature. 2009;457:97–101.
20. Kiel MJ, Yilmaz OH, Iwashita T, Yilmaz OH, Terhorst C, Morrison SJ. SLAM family receptors distinguish hematopoietic stem and progenitor cells and reveal endothelial niches for stem cells. Cell. 2005;121:1109–1121.
21. Raaijmakers MH. Niche contributions to oncogenesis: emerging concepts and implications for the hematopoietic system. Haematologica. 2011;96:1041–1048.
22. Walkley CR, Olsen GH, Dworkin S, et al. A microenvironment-induced myeloproliferative syndrome caused by retinoic acid receptor gamma deficiency. Cell. 2007;129:1097–1110.
23. Walkley CR, Shea JM, Sims NA, Purton LE, Orkin SH. Rb regulates interactions between hematopoietic stem cells and their bone marrow microenvironment. Cell. 2007;129:1081–1095.
24. Raaijmakers MH, Mukherjee S, Guo S, et al. Bone progenitor dysfunction induces myelodysplasia and secondary leukaemia. Nature. 2010;464:852–857.
25. Dong L, Yu WM, Zheng H, et al. Leukaemogenic effects of Ptpn11 activating mutations in the stem cell microenvironment. Nature. 2016;539:304–308.
26. Hooper AT, Butler JM, Nolan DJ, et al. Engraftment and reconstitution of hematopoiesis is dependent on VEGFR2-mediated regeneration of sinusoidal endothelial cells. Cell Stem Cell. 2009;4:263–274.
27. Doan PL, Russell JL, Himburg HA, et al. Tie2(+) bone marrow endothelial cells regulate hematopoietic stem cell regeneration following radiation injury. Stem Cells. 2013;31:327–337.
28. Butler JM, Nolan DJ, Vertes EL, et al. Endothelial cells are essential for the self-renewal and repopulation of Notch-dependent hematopoietic stem cells. Cell Stem Cell. 2010;6:251–264.
29. Gori JL, Butler JM, Chan YY, et al. Vascular niche promotes hematopoietic multipotent progenitor formation from pluripotent stem cells. J Clin Invest. 2015;125:1243–1254.
30. Feng Y, Liu M, Guo F, et al. Novel method to study mouse bone marrow endothelial cells in vivo and in vitro. Blood. 2012;120:617 (Abstract).
31. Staffas A, Karlsson C, Persson M, Palmqvist L, Bergo MO. Wild-type KRAS inhibits oncogenic KRAS-induced T-ALL in mice. Leukemia. 2015;29:1032–1040.
32. Ding L, Saunders TL, Enikolopov G, Morrison SJ. Endothelial and perivascular cells maintain haematopoietic stem cells. Nature. 2012;481:457–462.
33. Comazzetto S, Murphy MM, Berto S, Jeffery E, Zhao Z, Morrison SJ. Restricted hematopoietic progenitors and erythropoiesis require SCF from leptin receptor+ niche cells in the bone marrow. Cell Stem Cell. 2019;24:477–486.e6.
34. Forde A, Constien R, Grone HJ, Hammerling G, Arnold B. Temporal Cre-mediated recombination exclusively in endothelial cells using Tie2 regulatory elements. Genesis. 2002;33:191–197.
35. Li XM, Hu Z, Jorgenson ML, Slayton WB. High levels of acetylated low-density lipoprotein uptake and low tyrosine kinase with immunoglobulin and epidermal growth factor homology domains-2 (Tie2) promoter activity distinguish sinusoids from other vessel types in murine bone marrow. Circulation. 2009;120:1910–1918.
36. Alhamdoosh M, Law CW, Tian L, Sheridan JM, Ng M, Ritchie ME. Easy and efficient ensemble gene set testing with EGSEA. F1000Res. 2017;6:2010.
37. Lyubynska N, Gorman MF, Lauchle JO, et al. A MEK inhibitor abrogates myeloproliferative disease in Kras mutant mice. Sci Transl Med. 2011;3:76ra27.
38. Arranz L, Sanchez-Aguilera A, Martin-Perez D, et al. Neuropathy of haematopoietic stem cell niche is essential for myeloproliferative neoplasms. Nature. 2014;512:78–81.
39. Xu D, Liu X, Yu WM, et al. Non-lineage/stage-restricted effects of a gain-of-function mutation in tyrosine phosphatase Ptpn11 (Shp2) on malignant transformation of hematopoietic cells. J Exp Med. 2011;208:1977–1988.
40. Le DT, Kong N, Zhu Y, et al. Somatic inactivation of Nf1 in hematopoietic cells results in a progressive myeloproliferative disorder. Blood. 2004;103:4243–4250.
41. Acar M, Kocherlakota KS, Murphy MM, et al. Deep imaging of bone marrow shows non-dividing stem cells are mainly perisinusoidal. Nature. 2015;526:126–130.
42. Itkin T, Gur-Cohen S, Spencer JA, et al. Distinct bone marrow blood vessels differentially regulate haematopoiesis. Nature. 2016;532:323–328.
43. Zhou Y, He Y, Xing W, et al. An abnormal bone marrow microenvironment contributes to hematopoietic dysfunction in Fanconi anemia. Haematologica. 2017;102:1017–1027.
44. Drutskaya MS, Ortiz M, Liepinsh DJ, Kuprash DV, Nedospasov SA, Keller JR. Inhibitory effects of tumor necrosis factor on hematopoiesis seen in vitro are translated to increased numbers of both committed and multipotent progenitors in TNF-deficient mice. Exp Hematol. 2005;33:1348–1356.
45. Ishida T, Suzuki S, Lai CY, et al. Pre-transplantation blockade of TNF-alpha-mediated oxygen species accumulation protects hematopoietic stem cells. Stem Cells. 2017;35:989–1002.
46. Verstovsek S, Manshouri T, Pilling D, et al. Role of neoplastic monocyte-derived fibrocytes in primary myelofibrosis. J Exp Med. 2016;213:1723–1740.
47. Qiu J, Salama ME, Hu CS, Li Y, Wang X, Hoffman R. The characteristics of vessel lining cells in normal spleens and their role in the pathobiology of myelofibrosis. Blood Adv. 2018;2:1130–1145.
48. Li J, Yang S, Lu S, et al. Differential gene expression profile associated with the abnormality of bone marrow mesenchymal stem cells in aplastic anemia. PLoS One. 2012;7:e47764.

Supplemental Materials

Supplemental Methods

Generation of Tie2-CreER^{T2};KRas^{G12D};tdT Transgenic Mouse Lines. To generate an endothelial-specific inducible *Cre* line, previously described Tie2-CreER^{T2} mice were crossed with mice bearing the LSL-KRas^{G12D} mutation and the Rosa26-tdTomato transgene. Both the LSK-KRas^{G12D} and the Rosa26-tdTomato mice were obtained from Jackson lab. Tamoxifen was injected into Tie2CreERT2;tdTomato mice once/day for 3-5 days (Cayman Chemical 13258).

Histopathology. Mouse bones and spleens were fixed in 10% neutral buffered formalin, washed with PBS, and dehydrated in 70% ethanol. Paraffin embedding, microtomy, and staining with hematoxylin and eosin were performed by the Research Pathology Core at Cincinnati Children's Hospital Medical Center.

Colony-Forming Assays. Blood (100uL) or cells from bone marrow (2×10^4 cells) and spleen (2×10^5 cells) were isolated and then seeded in triplicates per 1mL of Methocult medium (M3434, StemCell Technologies) in a humidified 37°C, 5% carbon dioxide incubator. Colony-forming units were scored 7-10 days later using an inverted microscope.

Flow Cytometry and Cell Sorting. Multiparameter flow cytometry analysis was performed. Cells were first blocked with mouse BD Fc block™. Lineage markers CD45 (30-F11), Mac1 (M1/70), Gr1 (RB6-8C5), B220 (RA3-6B2), and CD3 (17A2) were used. For HSPC analysis, the following markers were used: Lineage-streptavidin, Sca-1 (D7), CD117 (2B8), CD135 (A2F10), and FC γ R III/II (93) were used. Data were collected on LSR II. The gating was done after the exclusion of dead cells, doublets, and debris. Cell sorting was done on the basis of CD31 + (MEC13.3) tdT+ using a FACS Aria cytometer. Antibodies were purchased mostly from Biolegend, with some from BD Biosciences or e-Bioscience.

Immunofluorescence Staining. Bone marrows were flushed from hind leg bones. They were then fixed in 4% paraformaldehyde, washed, permeabilized with 0.1% of Triton-X, washed further, and incubated with blocking buffer for at least 2 hours. Incubation with primary antibodies was done overnight at 4°C. The marrows were washed and incubated with the secondary antibodies, washed again, and then mounted with Prolong Diamond Antifade mountant (Thermofisher P36965). Images were acquired using a confocal microscope (Nikon).

For the localization studies, heart perfusion was performed with 4% paraformaldehyde and the bones were then harvested and fixed. Bones were embedded in optimum cutting temperature compound (Sakura® Finetek 4583) and snap frozen in liquid nitrogen. After sectioning, the bones were purified by melting the compound. The bones were briefly fixed again, permeabilized, and then incubated with primary antibodies for 1-3 days at 4°C. Secondary antibodies were added. The bone tissues were mounted in an antifade reagent. Images were then using a Zeiss or Leica confocal microscope. Data were analyzed using the Volocity image analysis software.

Transplantation. For our BoyJ CD45.1 donor cell transplantation into MxCre;KRas^{G12D} or control mice, 3 million donor cells from pooled donors were transplanted into lethally irradiated 6-10 weeks old adult recipient mice. To ensure Cre expression, the recipient mice were injected intraperitoneally with polyinosinic-polycytidylic acid (GE Healthcare Life Sciences 27473201) at a dose of 10μL/g of body weight 1-2 weeks post transplant every other day for 2 doses.

For our competitive transplant experiment, 2.5 million CD45.2 donor cells obtained from the bone marrow were transplanted alongside an equal number of host competitor cells (CD45.1) from at least 3 pooled donors into lethally irradiated mice by tail vein injections for competitive transplant. For secondary non-competitive transplant, 3 million cells from at least 2 pooled donors were transplanted into lethally irradiated recipients. Retro-orbital bleeds were performed monthly to assess for donor chimerism.

Immunoblotting. For immunoblots, cell lysates were made from sorted CD31+ tdT+ cells. The protein separation was done on a 4-15% polyacrylamide gel (Biorad) and the proteins were transferred to a PVDF membrane. Primary antibody incubation was done overnight. Secondary antibody incubation was done the next day and the protein bands were imaged using a Biorad ChemiDoc imager.

RNA Sequencing. CD31+ tdT+ cells were sorted directly into Qiazol (Qiagen). RNA was then isolated from the flow cytometry sorted cell populations using the Qiagen RNeasy Mini Kit, per the manufacturer's instructions. The RNA quality was determined using an Agilent Bioanalyzer. All samples used had an RNA integrity number (RIN) $\geq$ 9.30. 75bp paired-end reads were sequenced using Illumina Hiseq2500, and aligned to the mouse mm9 genome with TopHat. Differential gene expression was analyzed using the Cufflinks pipeline[49]. Gene set enrichment analysis was achieved using the EGSEA[36], and GSEA software[50].

Supplementary references

49. Trapnell C, Roberts A, Goff L, et al. Differential gene and transcript expression analysis of RNA-seq experiments with TopHat and Cufflinks. Nat Protoc. 2012;7:562–578.

50. Subramanian A, Tamayo P, Mootha VK, et al. Gene set enrichment analysis: a knowledge-based approach for interpreting genome-wide expression profiles. Proc Natl Acad Sci USA. 2005;102:15545-15550.

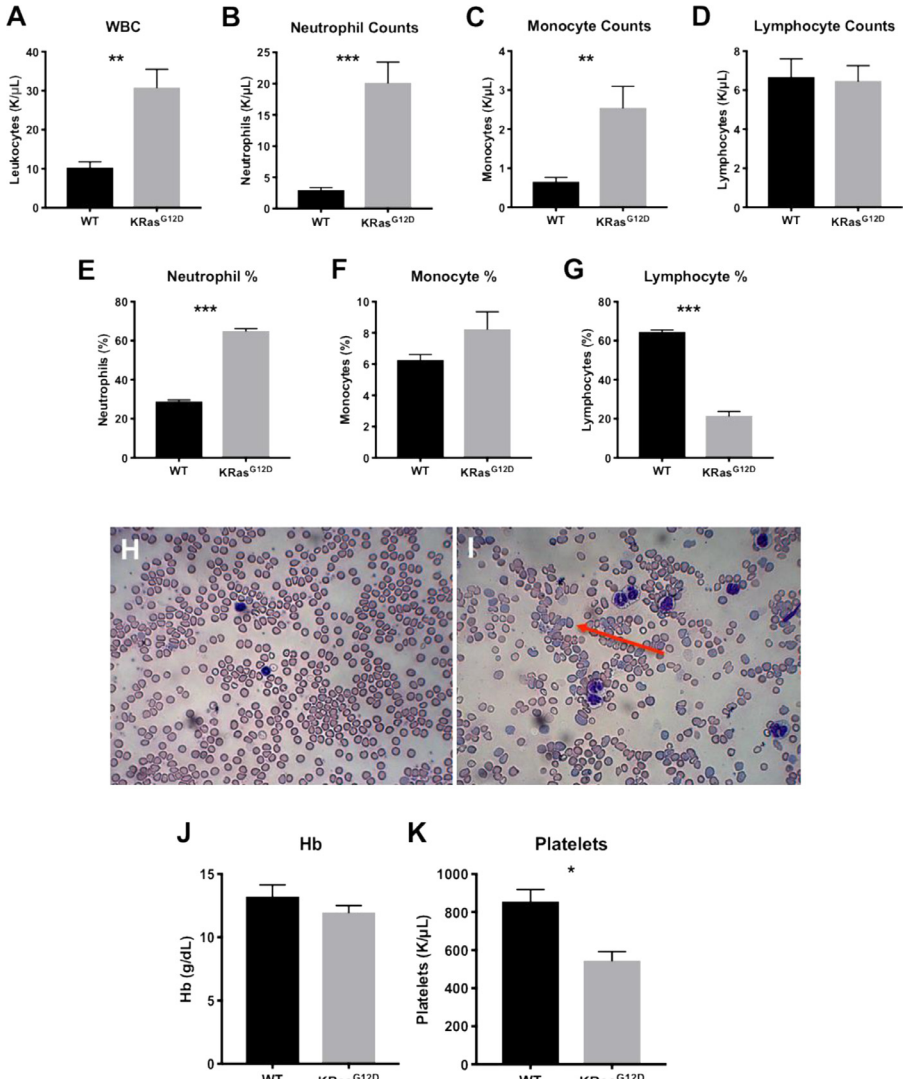

Supplementary Figure E1. KRas^{G12D} expression in the Mx1-cre driven mice leads to a MPD-like phenotype. MxCre;KRas^{G12D} or MxCre; KRas^{WT} mice were bled at 8 weeks of age. Complete blood counts were performed. **(A)** Total WBC counts, **(B)** Neutrophil counts, **(C)** Monocyte counts, **(D)** Lymphocyte counts. The mutant mice had significantly more **(E)** neutrophils, and **(F)** monocytes, and significantly **(G)** less lymphocytes. H&E staining showed **(H-I)** more leukocytes and polychromasia cells (indicated by the red arrowhead) in the blood. The MxCre; KRas^{G12D} mice had less **(J)** hemoglobin, and significantly less **(K)** platelet counts. n=3-5. *p<0.05, **p<0.01, and ***p<0.001.

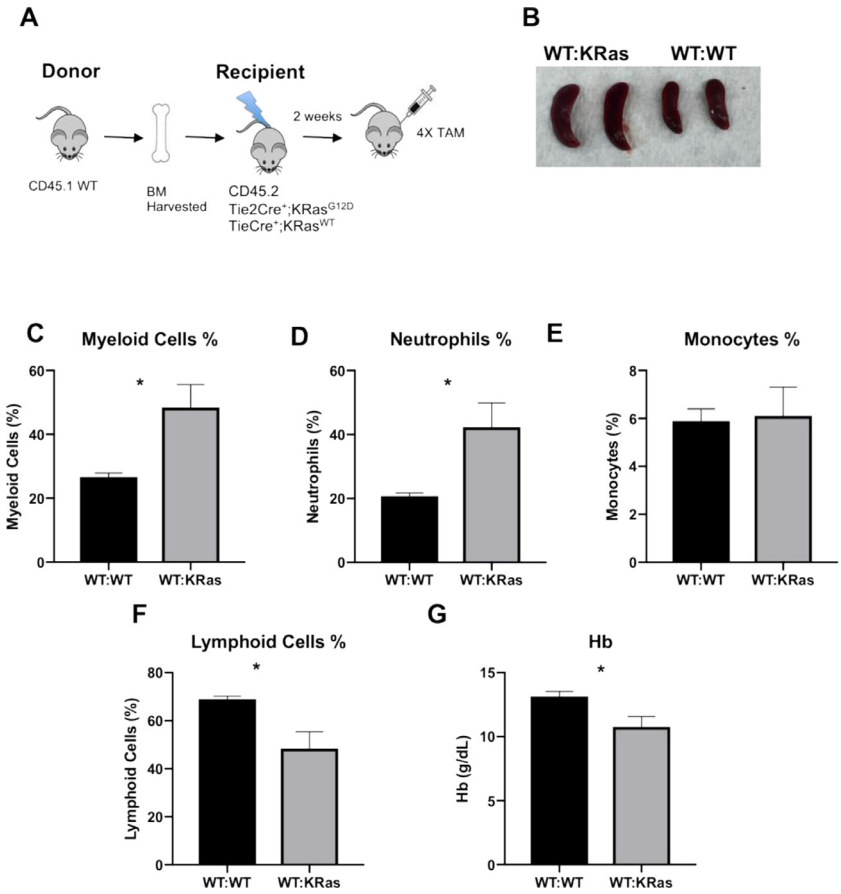

Supplementary Figure E2. Endothelial expression of KRas^{G12D} causes splenomegaly and a myeloid bias in a transplant setting. (A) Schematic of the transplant model. 3 million cells from CD45.1 BoyJ mice were transplanted into lethally irradiated Tie2Cre-ER;KRas^{G12D} mice (WT:KM) or Tie2Cre-ER;KRas^{WT} (WT:WT). The recipient mice were injected with Tamoxifen on 4 consecutive days 2 weeks after transplant. **(B)** The WT:KRas mice had enlarged spleens. At 16 weeks post transplant, they had **(C)** increased myeloid cell percentage, with a significant increase in the **(D)** neutrophil population, and no change in the **(E)** monocyte population. The mutant mice also had less **(F)** lymphoid cells and less **(G)** hemoglobin. n=6. *p<0.05.

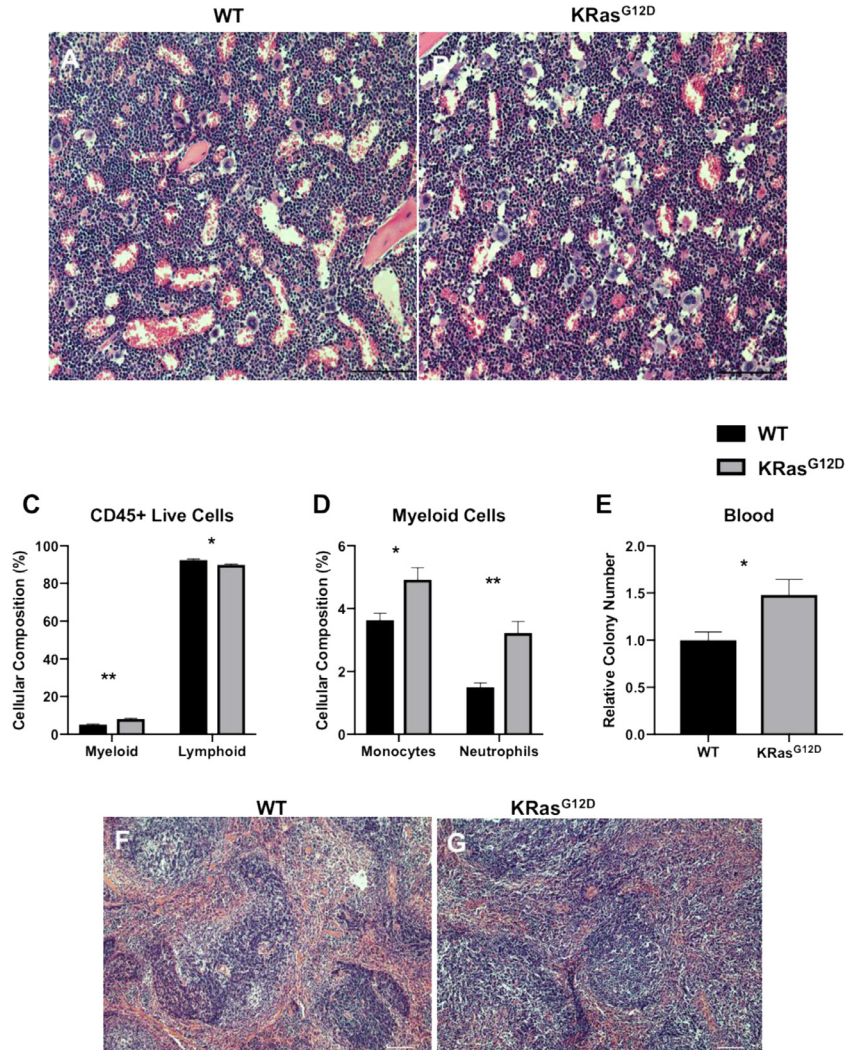

Supplementary Figure E3. Endothelial KRas^{G12D} expression does not significantly alter the BM but promotes extramedullary hematopoiesis. (A-B) H&E staining showed no major difference in the bone marrow. **(C-D)** FACS analysis at 13 weeks after TAM injections showed **(C)** a decrease in lymphoid cells and an increase in myeloid cells, especially in **(D)** neutrophils. n=3-4. **(E)** Colonies were scored 7-10 days after blood cells were plated in Methocult. KRas^{G12D} mice had an increased colony forming potential (n≥10). **(F-G)** H&E staining showed a minor difference in the spleen. *p<0.05, **p<0.01.